AIMS Mathematics, 8(7): 16191–16207
DOI: 10.3934/math.2023828
Received: 19 March 2023
Revised: 10 April 2023
Accepted: 12 April 2023
Published: 06 May 2023

http://www.aimspress.com/journal/Math

Research article

Adaptive backstepping position tracking control of quadrotor unmanned aerial vehicle system

Xia Song[1,2,*], **Lihua Shen**[3] **and Fuyang Chen**[1]

[1] College of Automation Engineering, Nanjing University of Aeronautics and Astronautics, Nanjing 211106, Jiangsu, China
[2] College of Science, Binzhou University, Binzhou 256600, Shandong, China
[3] Beijing Aerospace Automatic Control Institute, Beijing 100039, Beijing, China

* **Correspondence:** Email: songxia119@163.com.

Abstract: In this work, an adaptive backstepping position tracking control using neural network (NN) approximation mechanism is proposed with respect to the translational system of quadrotor unmanned aerial vehicle (QUAV). Concerning the translational system of QUAV, on the one hand, it does not satisfy the matching condition and is an under-actuation dynamic system; on the other hand, it is with strong nonlinearity containing some uncertainty. To achieve the control objective, an intermediary control is introduced to handle the under-actuation problem, then the backstepping technique is combined with NN approximation strategy, which is employed to compensate the uncertainty of the system. Compared with traditional adaptive methods, the proposed adaptive NN position control of QUAV can alleviate the computation burden effectively, because it only trains a scalar adaptive parameter instead of the adaptive parameter vector or matrix. Finally, according to Lyapunov stability proof and computer simulation, it is proved that the control tasks can be accomplished.

Keywords: quadrotor aerial robot; position control; translational system; backstepping control; neural network
Mathematics Subject Classification: 93B52, 93C10

1. Introduction

In recent decades, quadrotor unmanned aerial vehicle (QUAV) has been extensively applied to various fields, such as landscape mapping [1], agricultural survey [2], search and rescue operation [3], wild fire surveillance [4], due to some of its special features including low cost, simple structure, precise hovering, rapid maneuvering and vertical takeoff and landing [5]. To complete a control task, QUAV is driven via the lifted and propelled forces that are produced from the varying rotation

velocities of four rotors. Compared with conventional unmanned aerial vehicle (UAV), such as helicopter, fixed-wing aircraft, coaxial helicopter and twin rotor helicopter, QUAV has more excellent rotational agility and higher maneuverability owing to the special dynamic structure [6].

To control a QUAV system, the design of the position controller is most crucial. Nevertheless, finding a qualified position controller is a very challenging task because, on the one hand, the QUAV translational system contains some dynamic uncertainty, on the other hand, it is an under-actuated system [7]. For the sake of overcoming these challenges to control QUAV in autonomous flying and high maneuverability, lots of QUAV control approaches have been published in the literature, such as reinforcement learning optimized strategy [8], proportional-integral-derivative (PID) control [9], sliding mode control [10], linear quadratic regulator (LQR) control [11] and fuzzy logic (FL) control [12].

In the past decades, the backstepping technique has become a systematical and standard control methodology for the nonlinear high-order feedback system [13–16]. Since the technique does not require matching condition with regard to controlled system, it has a highlighting advantage which is the design flexibility compared with other control methods. Its design philosophy is to take many intermediary states as virtual controllers and to find the stable control law for them in accordance with the Lyapunov theorem [17, 18]. Ultimately, the ordered virtual control sequence will yield the actual control in the final step. From the process of design, the backstepping technique can ensure the goals of stabilizing and tracking. Particularly, it has become a popular technique in QUAV system control, and many interesting results are published, such as [19–22].

In the nonlinear control field, neural network (NN) has always been a popular tool to deal with the uncertain or unknown dynamics of systems [23–27]. In [23], in order to realize the nonlinear optimized control, reinforcement learning is constructed by employing the NN approximation. In [24], dynamic NNs are applied to the adaptive nonlinear identification and trajectory tracking. In [25], dynamic neural controls related with nonlinear system identification, nonlinear trajectory tracking, etc, are summarized. In [26], the optimized control of surface vessel is developed by using the adaptive NN. In [27], a robust asymptotic neuro observer is developed for the control of nonlinear system. In addition, fuzzy logic system (FLS) can also be as the universal approximator [28–30]. Therefore, NN or FLS control can be implemented to the complex nonlinear dynamic environment regardless of the completeness of system information.

However, these traditional NN adaptive controls, such as the above [23–27], require a large number of adaptive parameters for obtaining the desired accuracy of approximation. It is a stubborn defect which will result in a very heavy computational burden. As a result, the control will be also implemented with difficulty. Since QUAV translational system is modeled in a complex nonlinear strict-feedback dynamic form with some system uncertainty, it is feasible to apply the backstepping method and adaptive NN approximation strategy to the UAV control design. However, if the traditional adaptive NN strategies [23–27] are adopted in this control, there will be a large number of adaptive parameters because of the complex nonlinearity of the QUAV dynamic model.

Being motivated by the above, the paper proposes an adaptive NN backstepping tracking control approach for the QUAV translational system. The main contribution is introduced in the following.

With regard to the traditional adaptive NN control methods, such as [23–27], they usually update or train the NN weight vector or matrix directly. For increasing the NN approximation accuracy, the neuron number needs to become very big. As a result, the computation burden will be greatly increased.

However, different from these traditional methods, the proposed method needs to only update a scalar adaptive parameter that is the norm of weight matrix of adaptive NN, hence it can greatly alleviate the computation burden. This means that the proposed method can reduce the running cost and be easily applied in practice.

The paper's organization is introduced as follows. Section 2 is to introduce and describe two preliminaries of problem statement and neural network corresponding to two subsections. Section 3 is to share the main results, and it includes two subsections corresponding to control design and theorem proof. Section 4 is the simulation study, and a simulation example is utilized for illustrating QUAV position control. Section 5 is the conclusion of this article.

2. QUAV model statement and neural network formulation

2.1. Problem statement

With regard to a QUAV system whose basic configure is shown in Figure 1, it is usually modeled by two reference frames $E = \{x_e, y_e, z_e\}$ and $B = \{x_b, y_b, z_b\}$ that are, respectively, the earth fixed inertial and body fixed frames. Furthermore, the QUAV movement can be managed by the propeller forces $F_{i=1,2,3,4}$ produced from four rotors that are grouped into two pairs. The one pair is front and back rotors with clockwise rotation, and the other pair is left and right rotors with counterclockwise rotation.

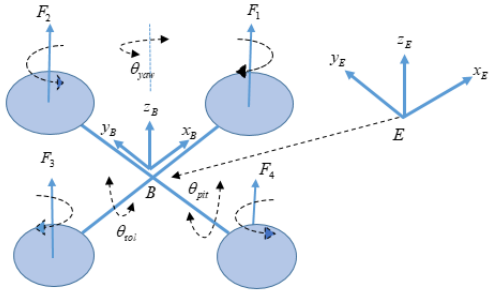

Figure 1. The basic configuration of QUAV.

In accordance with Newton-Euler formula, the QUAV position dynamic in the body fixed frame is expressed as

$$\bar{m}\dot{V} = -\bar{\Omega} \times \bar{m}V + F, \tag{2.1}$$

where $V = [V_x, V_y, V_z]^T \in \mathbf{R}^3$ and $\bar{\Omega} = [\bar{\Omega}_1, \bar{\Omega}_2, \bar{\Omega}_3]^T \in \mathbf{R}^3$ respectively denote the linear and rotational speeds, $\bar{m}$ is the QUAV mass, $\times$ denotes the vector product and $F \in \mathbf{R}^3$ is the total external force including gravity, thrust and other body forces [31, 32].

Let $\Theta(t) = [\theta_{rol}(t), \theta_{pit}(t), \theta_{yaw}(t)]^T \in \mathbf{R}^3$ signify the three Euler angles of roll, pitch and yaw, which can indicate the orientation of QUAV. Then the rotation matrix $R(\Theta) \in SO(3) \in \mathbf{R}^{3\times3}$ described in the following can be utilized to execute the coordinate transformation between frame B and frame E, where $SO(3)$ denotes the triaxial rotation group, i.e., $SO(3) = \{A|A^TA = I_3 \in \mathbf{R}^{3\times3}, det(A) = 1\}$.

$$R(\Theta) = \begin{bmatrix} c_{(\theta_{pit})}c_{(\theta_{yaw})} & s_{(\theta_{rol})}s_{(\theta_{pit})}c_{(\theta_{yaw})} - c_{(\theta_{rol})}s_{(\theta_{yaw})} & c_{(\theta_{rol})}s_{(\theta_{pit})}c_{(\theta_{yaw})} + s_{(\theta_{rol})}s_{(\theta_{yaw})} \\ c_{(\theta_{pit})}s_{(\theta_{yaw})} & s_{(\theta_{rol})}s_{(\theta_{pit})}s_{(\theta_{yaw})} + c_{(\theta_{rol})}c_{(\theta_{yaw})} & c_{(\theta_{rol})}s_{(\theta_{pit})}s_{(\theta_{yaw})} - s_{(\theta_{rol})}c_{(\theta_{yaw})} \\ -s_{(\theta_{pit})} & s_{(\theta_{rol})}c_{(\theta_{pit})} & c_{(\theta_{rol})}c_{(\theta_{pit})} \end{bmatrix}, \tag{2.2}$$

where $c_{(\cdot)}$ and $s_{(\cdot)}$ respectively denote two trigonometric functions $\cos(\cdot)$ and $\sin(\cdot)$.

By implementing the coordinate transformation from B to E, the translational dynamic equation (2.1) of QUAV can be re-expressed in inertial frame E as (referring to [31, 32])

$$\begin{aligned} \dot{\upsilon}_1(t) =& \upsilon_2(t), \\ \dot{\upsilon}_2(t) =& -\frac{1}{\bar{m}}K\upsilon_2(t) - \begin{bmatrix} 0 \\ 0 \\ g \end{bmatrix} + \frac{1}{\bar{m}}R(\Theta)\begin{bmatrix} 0 \\ 0 \\ 1 \end{bmatrix} u_p, \end{aligned} \tag{2.3}$$

where $\upsilon_1(t) = [x(t), y(t), z(t)] \in \mathbf{R}^3$ and $\upsilon_2(t) = [\dot{x}(t), \dot{y}(t), \dot{z}(t)]^T \in \mathbf{R}^3$ are, respectively, the position and velocity state vectors of QUAV in the inertial frame E, $u_p \in \mathbf{R}$ denotes the overall thrust force, g is the gravity acceleration and $K = diag\{K_x, K_y, K_z\}$ is the uncertain aerodynamic damping coefficient matrix [33].

Remark 1. *The rotational velocities $\omega_i(t)$, $i = 1, 2, 3, 4$ of four rotors are the direct control input of QUAV. Let $\tau = [\tau_{rol}, \tau_{pit}, \tau_{yaw}]^T$ denote the ideal attitude control, then u_p and τ have the following relations with $\omega_i(t)$, $i = 1, 2, 3, 4$.*

$$\begin{aligned} u_p =& \beta(\omega_1^2(t) + \omega_2^2(t) + \omega_3^2(t) + \omega_4^2(t)), \\ \tau_{rol} =& \beta l(\omega_2^2(t) - \omega_4^2(t)), \\ \tau_{pit} =& \beta l(-\omega_1^2(t) + \omega_3^2(t)), \\ \tau_{yaw} =& \gamma(\omega_1^2(t) - \omega_2^2(t) + \omega_3^2(t) - \omega_4^2(t)), \end{aligned} \tag{2.4}$$

where $\beta \in \mathbb{R}$ is the thrust factor, $\gamma \in \mathbb{R}$ is the drag factor and $l \in \mathbb{R}$ is the distance from rotors to the mass center. When u_p and τ are specified by designing, a power board will distribute the control input commands to four rotors by the relations. □

The control objective:

Depending on backstepping technique, design the adaptive NN control for the QUAV translational dynamic described in (2.3), such that 1) all control signals of the QUVA system are Semi-Globally Uniformly Ultimately Bounded (SGUUB) [34]; 2) the QUAV position states can track to the reference trajectories $\upsilon_r(t) = [x_{\upsilon r}(t), y_{\upsilon r}(t), z_{\upsilon r}(t)]^T \in \mathbf{R}^3$.

Assumption 1. *The predefined reference $\upsilon_r(t)$ and derivation $\dot{\upsilon}_r(t)$ are a bounded and measurable continuous time-function, hence they can be the valid information for the QUAV control design.*

Lemma 1. *[35] Regarding a positive continuous function $F(t) \in \mathbf{R}$, if it satisfies $\dot{F}(t) \leq -\alpha F(t) + \beta$ and has the bounded initial value $F(0)$, then it can meet the following inequality*

$$F(t) \leq e^{-\alpha t}F(0) + \frac{\beta}{\alpha}\left(1 - e^{-\alpha t}\right), \tag{2.5}$$

where α and β are two constants with $\alpha > 0$ and $\beta > 0$.

2.2. Neural network (NN)

NNs have universal approximation ability with respect to a continuous nonlinear function. With regard to a continuous nonlinear function $A(\chi) : \mathbf{R}^n \to \mathbf{R}^m$ on a predefined compact set, the NN approximation can be described as follows

$$A_{NN}(\chi) = \Psi^T \varpi(\chi), \tag{2.6}$$

where $\Psi \in \mathbf{R}^{p\times m}$ signifies the NN weight matrix with the neuron number p, $\varpi(\chi)$ is the basis function vector and $\varpi(\chi) = [\varpi_1(\chi), \cdots, \varpi_p(\chi)]^T \in \mathbf{R}^p$ with $\varpi_i(\chi) = \exp\left[-(\chi - \iota_i)^T(\chi - \iota_i)/2\right]$ where $\iota_i = [\iota_{i1}, \cdots, \iota_{in}]^T$ are the respective field centers, $i = 1, 2, \cdots, p$.

Let Ψ^* be the ideal NN weight. It is defined as

$$\Psi^* \triangleq \arg\min_{\Psi\in\mathbf{R}^{p\times m}} \left\{\sup_{\chi\in\Omega_\chi} \left\|A(\chi) - \Psi^T\varpi(\chi)\right\|\right\},$$

where Ω_χ is a compact set. Subsequently, in the light of the ideal NN approximation, the nonlinear function $A(\chi)$ can be rewritten as

$$A(\chi) = \Psi^{*T}\varpi(\chi) + \epsilon(\chi), \tag{2.7}$$

where $\epsilon(\chi) \in \mathbf{R}^m$ denotes the approximated error, which must be bounded [36].

3. Main results

3.1. Backstepping control design of QUAV position

Since the translational dynamic (2.3) associated with the position tracking control of QUAV is under-actuated, an intermediary control variable U is introduced with $U = 1/\bar{m}R(\Theta)\begin{bmatrix}0\\0\\1\end{bmatrix}u_p$, then the dynamical equation (2.3) can become

$$\begin{aligned}\dot{\upsilon}_1(t) =& \upsilon_2(t),\\ \dot{\upsilon}_2(t) =& -\frac{1}{\bar{m}}K\upsilon_2(t) - \begin{bmatrix}0\\0\\g\end{bmatrix} + U.\end{aligned} \tag{3.1}$$

Remark 2. *Applying the rotation matrix* (2.2)*, the relation of* $U = [U_x, U_y, U_z]^T \in \mathbf{R}^3$ *and* u_p *can be described as*

$$\begin{aligned}U_x =& \left(c_{(\theta_{rol})}s_{(\theta_{pit})}c_{(\theta_{yaw})} + s_{(\theta_{rol})}s_{(\theta_{yaw})}\right)\frac{u_p}{\bar{m}},\\ U_y =& \left(c_{(\theta_{rol})}s_{(\theta_{pit})}s_{(\theta_{yaw})} - s_{(\theta_{rol})}c_{(\theta_{yaw})}\right)\frac{u_p}{\bar{m}},\\ U_z =& c_{(\theta_{rol})}c_{(\theta_{pit})}\frac{u_p}{\bar{m}}.\end{aligned} \tag{3.2}$$

By solving (3.2), the actual control u_p can be obtained as (referring to [32])

$$u_p = \bar{m}(U_x^2 + U_y^2 + U_z^2)^{\frac{1}{2}}. \tag{3.3}$$

Using the desired position trajectory $\upsilon_r(t) = [x_{\upsilon r}(t), y_{\upsilon r}(t), z_{\upsilon r}(t)]^T \in \mathbf{R}^3$, the position tracking errors are defined as $e_1(t) = \upsilon_1 - \upsilon_r$ and $e_2(t) = \upsilon_2 - \alpha_e$, where $\alpha_e \in \mathbf{R}^3$ is the virtual control that is specified later. From (3.1), the error dynamics can be obtained as

$$\begin{aligned} \dot{e}_1(t) =& \upsilon_2(t) - \dot{\upsilon}_r(t), \\ \dot{e}_2(t) =& -\frac{1}{\bar{m}} K\upsilon_2(t) - \begin{bmatrix} 0 \\ 0 \\ g \end{bmatrix} - \dot{\alpha}_e + U. \end{aligned} \tag{3.4}$$

According to Assumption 1, the QUAV system is under the suitable attitude, then the QUAV position tracking control can be derived from the following 2-step backstepping.

Step 1. Applying the coordinate transformation $e_2(t) = \upsilon_2(t) - \alpha_e$, the $1st$ error dynamic in (3.4) can become

$$\dot{e}_1(t) = \alpha_e + e_2(t) - \dot{\upsilon}_r(t). \tag{3.5}$$

The virtual controller α_e is given as

$$\alpha_e = -\kappa_1 e_1(t) + \dot{\upsilon}_r(t), \tag{3.6}$$

where κ_1 is the positive gain parameter.

Corresponding to this backstepping step, consider the following Lyapunov function

$$L_1(t) = \frac{1}{2} e_1^T(t) e_1(t). \tag{3.7}$$

Along (3.5), its time derivation can be calculated as

$$\dot{L}_1(t) = e_1^T(t)(\alpha_e + e_2(t) - \dot{\upsilon}_r(t)). \tag{3.8}$$

Substitute (3.6) into (3.8) to have

$$\dot{L}_1(t) = -\kappa_1 e_1^T e_1 + e_1^T e_2. \tag{3.9}$$

According to Young's inequality and Cauchy–Schwartz inequality, the following one can be got

$$e_1^T(t) e_2(t) \leq \frac{1}{2} e_1^T(t) e_1(t) + \frac{1}{2} e_2^T(t) e_2(t). \tag{3.10}$$

Inserting (3.10) into (3.9), we can get

$$\begin{aligned}\dot{L}_1(t) \leq & -\Big(\kappa_1 - \frac{1}{2}\Big)e_1^T(t)e_1(t) + \frac{1}{2}e_2^T(t)e_2(t) \\ = & -(2\kappa_1 - 1)L_1(t) + \frac{1}{2}e_2^T(t)e_2(t). \end{aligned} \tag{3.11}$$

Step 2. This is the final backstepping step. The actual QUAV position control based on NN approximation mechanism is derived in this step.

The velocity error dynamic of (3.4) can be rewritten as

$$\dot{e}_2(t) = f(\upsilon_2, \dot{\alpha}_e) + U, \tag{3.12}$$

where $f(\upsilon_2, \dot{\alpha}_e) = -\frac{1}{\tilde{m}}K\upsilon_2(t) - \begin{bmatrix}0\\0\\g\end{bmatrix} - \dot{\alpha}_e$.

From the dynamic equation (3.12), the position controller needs to involve the function $f(\upsilon_2, \dot{\alpha}_e)$. Because the function $f(\upsilon_2, \dot{\alpha}_e)$ contains the uncertain parameter K, it is not qualified for the design of controller. However, since the function is continuous, NNs can be employed to approximate it over a predefined compact set $\Omega_u \in \mathbf{R}^3$ by the following form

$$f(\upsilon_2, \dot{\alpha}_e) = \Psi^{*T}\varpi(\upsilon_2, \dot{\alpha}_e) + \epsilon(\upsilon_2, \dot{\alpha}_e), \tag{3.13}$$

where $\Psi^* \in \mathbf{R}^{m\times 3}$ is the optimal NN weight, $\varpi(\upsilon_2, \dot{\alpha}_e) \in \mathbf{R}^m$ is the basis function vector and $\epsilon(\upsilon_2, \dot{\alpha}_e) \in \mathbf{R}^3$ is the approximation error. There m is the number of neural neuron.

Since the optimal weight matrix Ψ^* is a constant matrix but unknown, it needs to be adaptively estimated for the design of controller. Further, the adaptive QUAV position control is designed as

$$U = -\kappa_2 e_2(t) - \gamma\hat{\psi}(t)\|\varpi(\upsilon_2, \dot{\alpha}_e)\|^2 e_2(t), \tag{3.14}$$

where $\hat{\psi}(t) \in \mathbf{R}$ is the adaptive estimation of optimal NN weight's norm $\psi^* = \|\Psi^*\|^2$ and is updated via the following rule

$$\dot{\hat{\psi}}(t) = \gamma\|\varpi(\upsilon_2, \dot{\alpha}_e)\|^2\|e_2(t)\|^2 - \beta\hat{\psi}(t), \tag{3.15}$$

where κ_2, γ and β are the positive design parameters.

Remark 3. *Since backstepping technique can release the matching condition in a nonlinear control design, it has become a popular technique in the QUAV control recently [37–40]. In this work, for handling the unknown or uncertain dynamic problem of the QUAV position control, the backstepping technique is combined with the adaptive NN approximation strategy, because NN has many remarkable and significant features, such as universal approximation ability, good robustness and simple structure.*

However, the above adaptive control (3.14) *with learning law* (3.15) *has a key difference compared with the traditional adaptive NN control methods, such as [23–27]. In these traditional control methods, their adaptive laws are to train the NN weight vector or matrix. If the neuron number becomes very big for increasing the accuracy of the NN approximation, the computation burden will be greatly increased. While the learning law* (3.15) *of the proposed adaptive control is to only train a scalar adaptive parameter rather than vector or matrix. Therefore, the computation burden can be greatly alleviated.*

The whole Lyapunov function associated with this backstepping step is chosen as

$$L_2(t) = L_1(t) + \frac{1}{2}e_2^T(t)e_2(t) + \frac{1}{2}\tilde{\psi}^2(t), \tag{3.16}$$

where $\tilde{\psi}(t)$ is the NN weight error with $\tilde{\psi}(t) = \hat{\psi}(t) - \psi^*$.

According to (3.12) and (3.15), the time derivative of $L_2(t)$ can be calculated as

$$\begin{aligned}\dot{L}_2(t) =& \dot{L}_1(t) + e_2^T(t)\left(f(\upsilon_2, \dot{\upsilon}_r) + U\right) \\ &+ \tilde{\psi}(t)(\gamma\|\varpi(\upsilon_2, \dot{\upsilon}_r)\|^2\|e_2(t)\|^2 - \beta\hat{\psi}(t)).\end{aligned} \tag{3.17}$$

Substituting (3.13) into (3.17), there is the following result

$$\begin{aligned}\dot{L}_2(t) =& \dot{L}_1(t) - e_2^T(t)\Big(\Psi^{*T}\varpi(\upsilon_2, \dot{\upsilon}_r) + \epsilon(\upsilon_2, \dot{\upsilon}_r) + U\Big) \\ &+ \tilde{\psi}(t)\Big(\gamma\|\varpi(\upsilon_2, \dot{\upsilon}_r)\|^2\|e_2(t)\|^2 - \beta\hat{\psi}(t)\Big).\end{aligned} \tag{3.18}$$

According to Young's inequality, there are the following two inequalities

$$\begin{aligned}-e_2^T(t)\Psi^{*T}\varpi(\upsilon_2, \dot{\upsilon}_r) &\le \gamma\|e_2(t)\|^2\psi^*\|\varpi(\upsilon_2, \dot{\upsilon}_r)\|^2 + \frac{1}{\gamma}, \\ -e_2^T(t)\epsilon(\upsilon_2, \dot{\upsilon}_r) &\le \frac{1}{2}e_2^T(t)e_2(t) + \frac{1}{2}\epsilon^T(\upsilon_2, \dot{\upsilon}_r)\epsilon(\upsilon_2, \dot{\upsilon}_r),\end{aligned} \tag{3.19}$$

where $\psi^* = \|\Psi^*\|^2$.

Using the above inequalities (3.19), the (3.18) can be re-described as

$$\begin{aligned}\dot{L}_2(t) \le& \dot{L}_1(t) + \frac{1}{2}e_2^T(t)e_2(t) + \gamma\|e_2(t)\|^2\psi^*\|\varpi(\upsilon_2, \dot{\upsilon}_r)\|^2 \\ &+ e_2^T(t)U + \tilde{\psi}(t)\Big(\gamma\|\varpi(\upsilon_2, \dot{\upsilon}_r)\|^2\|e_2(t)\|^2 - \beta\hat{\psi}(t)\Big) \\ &+ \frac{1}{2}\|\epsilon(\upsilon_2, \dot{\upsilon}_r)\|^2 + \frac{1}{\gamma}.\end{aligned} \tag{3.20}$$

Implementing the position control (3.14), the above inequality can become

$$\begin{aligned}\dot{L}_2(t) \le& \dot{L}_1(t) - (\kappa_2 - \frac{1}{2})e_2^T(t)e_2(t) - \gamma\tilde{\psi}(t)\|e_2(t)\|^2\|\varpi(\upsilon_2, \dot{\upsilon}_r)\|^2 \\ &+ \tilde{\psi}(t)\Big(\gamma\|\varpi(\upsilon_2, \dot{\upsilon}_r)\|^2\|e_2(t)\|^2 - \beta\hat{\psi}(t)\Big) \\ &+ \frac{1}{2}\|\epsilon(\upsilon_2, \dot{\upsilon}_r)\|^2 + \frac{1}{\gamma}.\end{aligned} \tag{3.21}$$

Further, the equation (3.20) can be transformed into the following one,

$$\dot{L}_2(t) = \dot{L}_1(t) - (\kappa_2 - \frac{1}{2})e_2^T e_2 - \beta\tilde{\psi}(t)\hat{\psi}(t) + \frac{1}{2}\|\epsilon(\upsilon_2, \dot{\upsilon}_r)\|^2 + \frac{1}{\gamma}. \tag{3.22}$$

Using $\tilde{\psi}(t) = \hat{\psi}(t) - \psi^*$, there is the following equation

$$\begin{aligned} -\tilde{\psi}(t)\hat{\psi}(t) &= -\frac{1}{2}\tilde{\psi}^2(t) - \frac{1}{2}\hat{\psi}^2(t) + \frac{1}{2}\psi^{*2} \\ &\leq -\frac{1}{2}\tilde{\psi}^2(t) + \frac{1}{2}\psi^{*2}. \end{aligned} \tag{3.23}$$

Substituting (3.23) into (3.22), there is

$$\begin{aligned} \dot{L}_2(t) \leq & \dot{L}_1(t) - (\kappa_2 - \frac{1}{2})e_2^T(t)e_2(t) - \frac{\beta}{2}\tilde{\psi}^2(t) \\ & + \frac{\beta}{2}\psi^{*2} + \frac{1}{2}\|\epsilon(\upsilon_2, \dot{\upsilon}_r)\|^2 + \frac{1}{\gamma}. \end{aligned} \tag{3.24}$$

Substitute the result (3.11) into (3.24) to have

$$\begin{aligned} \dot{L}_2(t) \leq & -(2\kappa_1 - 1)L_1(t) - \Big(\kappa_2 - 1\Big)e_2^T(t)e_2(t) \\ & - \frac{\beta}{2}\tilde{\psi}^2(t) + c, \end{aligned} \tag{3.25}$$

where c is the boundedness of term $\frac{\beta}{2}\psi^{*2} + \frac{1}{2}\|\epsilon(\upsilon_2, \dot{\alpha}_e)\|^2 + \frac{1}{\gamma}$.

Let $a = \min\{2\kappa_1 - 1, 2\kappa_2 - 2, \beta\}$, then the following inequality can be got from (3.25)

$$\dot{L}_2(t) \leq -aL_2(t) + c. \tag{3.26}$$

3.2. Main conclusion

Theorem 1. *Refer to the QUAV translation system* (2.3) *under suitable attitude, if the NN backstepping position control is implemented via* (3.6) *and* (3.14) *with the updating law* (3.15)*, and the design parameters can meet the conditions* $\kappa_1 > 1/2$*,* $\kappa_2 > 1$*,* $\beta > 0$ *and* $\gamma > 0$*, then the backstepping control can be guaranteed that*

1). all control variables are SGUUB;

2). the QUAV position state $\upsilon_1(t)$ *can track the desired reference* $\upsilon_r(t)$ *under an ideal accuracy.*

Proof of Theorem 1. According to Lemma 1, from (3.26), there is the following one

$$L_2(t) \leq e^{-at}L_2(0) + \frac{c}{a}\left(1 - e^{-at}\right). \tag{3.27}$$

In the light of the above inequality, it can conclude that all error signals are SGUUB, and both tracking errors $e_1(t)$ and $e_2(t)$ can arrive in a small zero neighborhood by selecting the designed parameters large enough.

Remark 4. *The QUAV translational dynamic* (2.3) *is assumed to accompany with a corrected attitude. In fact, the QUAV attitude control law can be designed similar with the above position control, and it is introduced in the appendix section.*

4. Simulation

In this section, the proposed backstepping position control is further demonstrated by a numerical QUAV system simulation in Matlab environment. The UAV model parameters are $\bar{I}_x = 4.85\times10^{-3}(kg\cdot m^2)$, $\bar{I}_y = 4.85\times10^{-3}(kg\cdot m^2)$, $\bar{I}_z = 8.81\times10^{-3}(kg\cdot m^2)$, $\bar{m} = 0.5(kg)$ and $g = 9.81(m/s^2)$, which refer to reference [19]. The NN is set with 16 nodes, and the centers ι_i are equally distributed in the space $[-9, 9]$.

There are the desired position trajectory $\upsilon_r = [5s_{(t)}, 5c_{(t)}, t]^T$ and the initial position set as $\upsilon_r(0) = [0.35, 0.35, 0.35]^T$. The attitude signals for assisting position control are assumed to be produced from the following equation (referring to [8])

$$\begin{aligned}\theta_{yaw} =&\pi/4,\\ \theta_{rol}(t) =& \arcsin\Big(\bar{m}\frac{U_x s_{(\theta_{yaw})} - U_y c_{(\theta_{yaw})}}{u_p}\Big),\\ \theta_{pit}(t) =& \arctan\Big(\frac{U_x c_{(\theta_{yaw})} + U_y s_{(\theta_{yaw})}}{U_z}\Big).\end{aligned} \tag{4.1}$$

The virtual control corresponding to (3.6) of the $1st$ backstepping step chooses the design parameter $\kappa_1 = 18$. The actual control corresponding to (3.14) of the $2nd$ backstepping step chooses the design parameter $\kappa_2 = 12$. Corresponding to (3.15), the updating law is set with the parameters $\gamma = 3$ and $\beta = 2$. The initial values are set as $\upsilon_1(0) = 0.3$, $\upsilon_2(0) = 0.5$ and $\hat{\psi}(0) = 0.6$.

The run results of simulation are displayed by Figures 2–5. Figure 2 shows the tracking performance, and it shows that QUAV position states track the desired position trajectory. Figures 3 and 4 show the tracking errors of two backstepping steps respectively. The boundedness of NN weight is displayed by Figure 5. Figures 2–5 further certify that the proposed QUAV position control method can finally complete the control tasks.

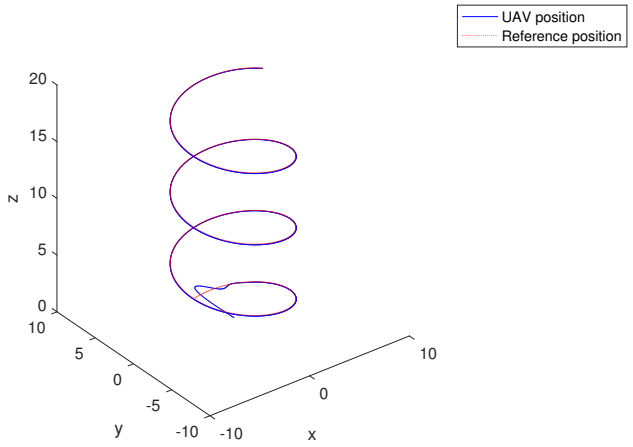

Figure 2. The QUAV position tracking performance.

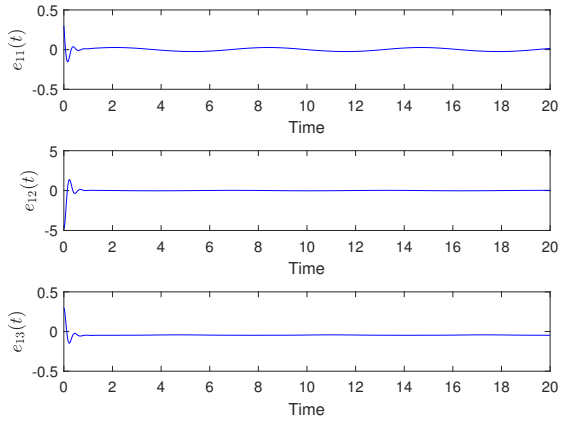

Figure 3. The tracking error of 1st backstepping step.

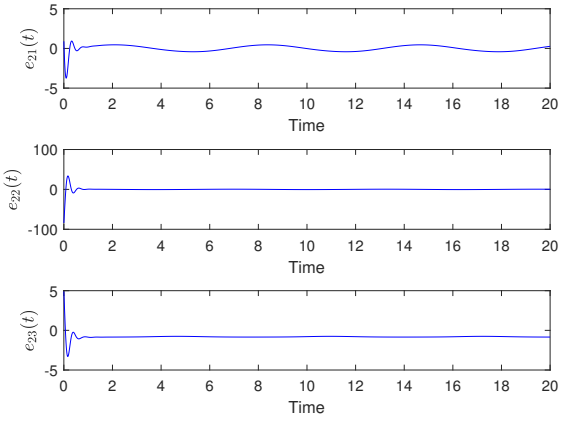

Figure 4. The tracking error of 2nd backstepping step.

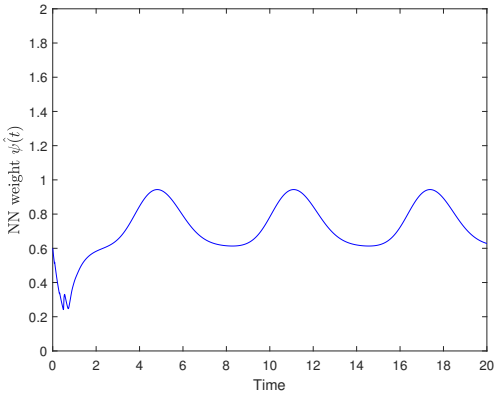

Figure 5. The boundedness of NN weight.

In order to show advantage of the proposed method, the traditional adaptive NN method of reference [35] is implemented to the above QUAV position control, and the results are shown in Figures 6 and 7. By comparing the two Figures 5 and 7, it can be concluded that, in the similar control performance, the proposed method can yield the smaller amplitude in adaptive NN weight than the traditional adaptive NN method of reference [35].

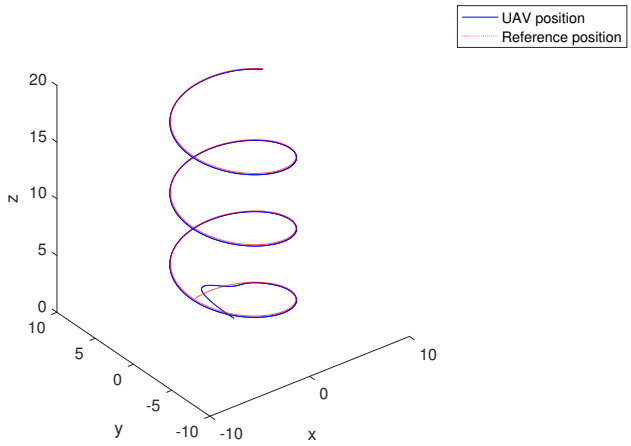

Figure 6. The QUAV position tracking performance of using the adaptive NN method of reference [35].

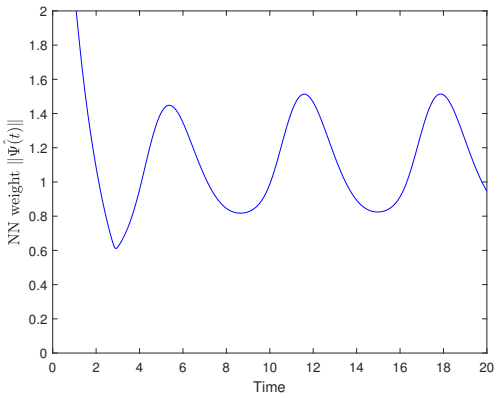

Figure 7. The NN weight of using the adaptive NN method of reference [35].

5. Conclusions and future works

By combining the backstepping technique with adaptive NN approximation strategy, a position tracking control scheme of QUAV system is developed. Since the translational system of QUAV is modeled by the under-actuated nonlinear strict feedback form with some uncertainty, the control design is very interesting and challenging. In order to achieve the control, an intermediary control is introduced so that backstepping can be smoothly implemented, then NN approximation is employed

to compensate the system uncertainty. Since only a scalar adaptive parameter is updated for the NN approximation, the control method is with a less computation burden. In accordance with the stability analysis and simulation, it is certified that this proposed QUAV position control algorithm can achieve the control objective.

In our future work, the main study will be focused on the multi-QUAV control, and we will develop the method of QUAV formation control. Different from the single QUAV control, the multi-QUAV control aims to make the cooperation of multiple QUAVs by using the state coupling controller, and it can surpass the ability of multiple single QUAVs.

Acknowledgments

This work is supported in part by national natural science foundation of China under grant No.62173179, in part by the Science and Technology Foundations of Shandong Province under Grant No.J18KB105, in part by the Natural Science Foundation of Shandong Province under Grant ZR2021MF088.

Conflict of interest

No potential conflict of interest was reported by the authors.

References

1. P. Rodriguez-Gonzalvez, D. Gonzalez-Aguilera, G. Lopez-Jimenez, I. Picon-Cabrera, Imagebased modeling of built environment from an unmanned aerial system, *Automat. Const.*, **48** (2014), 44–52. http://dx.doi.org/10.1016/j.autcon.2014.08.010
2. J. Senthilnath, A. Dokania, M. Kandukuri, K. N. Ramesh, G. Anand, S. N. Omkar, Detection of tomatoes using spectral-spatial methods in remotely sensed rgb images captured by uav, *Biosyst. Eng.*, **146** (2016), 16–32. http://dx.doi.org/10.1016/j.biosystemseng.2015.12.003
3. A. Ryan, J. K. Hedrick, A mode-switching path planner for uav-assisted search and rescue, In: *Proceedings 44th IEEE Confrences Decision and Control*, 2005, 1471–1476. http://dx.doi.org/10.1109/CDC.2005.1582366
4. K. Alexis, G. Nikolakopoulos, A. Tzes, L. Dritsas, Coordination of Helicopter UAVs for Aerial Forest-Fire Surveillance, *Appl. Intell. Control Eng. Systems*, **39** (2009), 169–193. http://dx.doi.org/10.1007/978-90-481-3018-4_7
5. X. Liang, Y. Fang, N. Sun, H. Lin, Dynamics analysis and time-optimal motion planning for unmanned quadrotor transportation systems, *Mechatronics*, **50** (2018), 16–29. http://dx.doi.org/10.1016/j.mechatronics.2018.01.009
6. H. Liu, X. Wang, Y. Zhong, Dynamics analysis and time-optimal motion planning for unmanned quadrotor transportation systems, *IEEE T. Ind. Inform.*, **11** (2017), 406–415. http://dx.doi.org/10.1109/TII.2015.2397878
7. S. Gupte, P. I. T. Mohandas, J. M. Conrad, A survey of quadrotor unmanned aerial vehicles, In: *2012 Proceedings of IEEE Southeastcon,* 2012, 1–6. http://dx.doi.org/10.1109/SECon.2012.6196930

8. G. Wen, W. Hao, W. Feng, K. Gao, Optimized backstepping tracking control using reinforcement learning for quadrotor unmanned aerial vehicle system, *IEEE T. Syst. Man Cy. Syst.*, **52** (2022), 5004–5015. http://dx.doi.org/10.1109/TSMC.2021.3112688
9. A. L. Salih, M. Moghavvemi, H. A. F. Mohamed, K. S. Gaeid, Modelling and pid controller design for a quadrotor unmanned air vehicle, In: *2010 IEEE International Conference on Automation, Quality and Testing, Robotics (AQTR),* **1** (2010), 1–5. http://dx.doi.org/10.1109/AQTR.2010.5520914
10. R. Xu, U. Ozguner, Sliding mode control of a quadrotor helicopter, In: *Proceedings of the 45th IEEE Conference on Decision and Control*, (2006), 4957–4962. https://doi.org/10.1109/CDC.2006.377588
11. P. Castillo, R. Lozano, A. Dzul, Stabilization of a mini rotorcraft with four rotors, *IEEE Control Syst.*, **25** (2005), 45–55. https://doi.org/10.1109/IROS.2004.1389815
12. M. Santos, V. Lopez, F. Morata, Intelligent fuzzy controller of a quadrotor, In: *2010 IEEE International Conference on Intelligent Systems and Knowledge Engineering*, 2010, 141–146. https://doi.org/10.1109/ISKE.2010.5680812
13. G. Wen, S. S. Ge, F. Tu, Optimized backstepping for tracking control of strict-feedback systems, *IEEE T. Neur. Net. Lear. Syst.*, **29** (2018), 3850–3862. http://dx.doi.org/10.1109/TNNLS.2018.2803726
14. A. Karimi, A. Feliachi, Decentralized adaptive backstepping control of electric power systems, *Electr. Pow. Syst. Res.*, **78** (2008), 484–493. http://dx.doi.org/10.1016/j.epsr.2007.04.003
15. Q. Xie, Z. Han, H. Kang, Adaptive backstepping control for hybrid excitation synchronous machine with uncertain parameters, *Expert Syst. Appl.*, **37** (2010), 7280–7284. http://dx.doi.org/10.1016/j.eswa.2010.03.038
16. G. Wen, C. L. P. Chen, S. S. Ge, Simplified optimized backstepping control for a class of nonlinear strict-feedback systems with unknown dynamic functions, *IEEE T. Cybernetics*, **51** (2021), 4567–4580. http://dx.doi.org/10.1109/TCYB.2020.3002108
17. R. Sakthivel, A. Parivallal, N. Huy Tuan, S. Manickavalli, Nonfragile control design for consensus of semi-markov jumping multiagent systems with disturbances, *Int. J. Adapt. Control Signal Proc.*, **35** (2021), 1039–1061. http://dx.doi.org/10.1002/acs.3245
18. A. Parivallal, R. Sakthivel, C. Wang, Guaranteed cost leaderless consensus for uncertain markov jumping multi-agent systems, *J. Exp. Theor. Artif. Int.*, **35** (2023), 257–273. http://dx.doi.org/10.1080/0952813X.2021.1960631
19. M. A. Mohd Basri, A. R. Husain, K. A. Danapalasingam, Enhanced backstepping controller design with application to autonomous quadrotor unmanned aerial vehicle, *J. Intell. Robot. Syst.*, **79** (2015), 295–321. http://dx.doi.org/10.1007/s10846-014-0072-3
20. T. Madani, A. Benallegue, Backstepping control for a quadrotor helicopter, In: *IEEE/RSJ International Conference on Intelligent Robots & Systemn*, 2006, 9419317. http://dx.doi.org/10.1109/IROS.2006.282433
21. T. Madani, A. Benallegue, Backstepping sliding mode control applied to a miniature quadrotor flying robot, In: *IECON 2006-32nd Annual Conference on IEEE Industrial Electronics*, 2006, 9430817. http://dx.doi.org/10.1109/IECON.2006.347236

22. T. Madani, A. Benallegue, Control of a quadrotor mini-helicopter via full state backstepping technique, In: *Proceedings of the 45th IEEE Conference on Decision and Control*, 2006, 9409085. http://dx.doi.org/10.1109/CDC.2006.377548

23. G. Wen, C. L. P. Chen, S. S. Ge, H. Yang, X. Liu, Optimized adaptive nonlinear tracking control using actor-critic reinforcement learning strategy, *IEEE T. Ind. Inform.*, **15** (2019), 4969–4977. http://dx.doi.org/10.1109/TII.2019.2894282

24. A. Poznyak, W. Yu, E. Sanchez, J. Perez, Nonlinear adaptive trajectory tracking using dynamic neural networks, *IEEE T. Neur. Net.*, **10** (1999), 1402–1411. http://dx.doi.org/10.1109/72.809085

25. A. S. Poznyak, W. Yu, E. N. Sanchez, J. P. Perez, Stability analysis of dynamic neural control, *Expert Syst. Appl.*, 14 (1998), 227–236. http://dx.doi.org/10.1016/S0957-4174(97)00072-9

26. G. Wen, S. S. Ge, C. L. P. Chen, F. Tu, S. Wang, Adaptive tracking control of surface vessel using optimized backstepping technique, *IEEE T. Cybernetics*. **49** (2019), 3420–3431. http://dx.doi.org/10.1109/TCYB.2018.2844177

27. A. Poznyak, W. Yu, Robust asymptotic neuro-observer with time delay term, *J. Robust Nonlin. Control*, **10** (2000), 535–559.

28. G. Wen, C. L. P. Chen, J. Feng, N. Zhou, Optimized multi-agent formation control based on an identifier-actor-critic reinforcement learning algorithm, *IEEE T. Fuzzy Syst.*, **26** (2018), 2719–2731. http://dx.doi.org/10.1109/TFUZZ.2017.2787561

29. Y. J. Liu, W. Wang, S. C. Tong, Y. S. Liu, Robust adaptive tracking control for nonlinear systems based on bounds of fuzzy approximation parameters, *IEEE T. Syst. Man Cy. A*, **40** (2010), 170–184. http://dx.doi.org/10.1109/TSMCA.2009.2030164

30. X. Shao, S. Tong, Adaptive fuzzy prescribed performance control for mimo stochastic nonlinear systems, *IEEE Access*, **6** (2018), 76754–76767. http://dx.doi.org/10.1109/ACCESS.2018.2882634

31. S. Islam, P. X. Liu, A. El Saddik, Nonlinear adaptive control for quadrotor flying vehicle, *Nonlinear Dynam.*, **78** (2014), 117–133. http://dx.doi.org/10.1007/s11071-014-1425-y

32. F. Kendoul, Z. Yu, K. Nonami, Guidance and nonlinear control system for autonomous flight of minirotorcraft unmanned aerial vehicles, *J. Field Robot.*, **27** (2010), 311–334. http://dx.doi.org/10.1002/rob.20327

33. B. Zhao, B. Xian, Y. Zhang, X. Zhang, Nonlinear robust adaptive tracking control of a quadrotor uav via immersion and invariance methodology, *IEEE T. Ind. Electron.*, **62** (2015), 2891–2902. http://dx.doi.org/10.1109/TIE.2014.2364982

34. G. Wen, S. S. Ge, F. Tu, Optimized backstepping for tracking control of strict-feedback systems, *IEEE T. Neural Net. Learning Syst.*, **29** (2018), 3850–3862. http://dx.doi.org/10.1109/TNNLS.2018.2803726

35. G. X. Wen, C. L. P. Chen, Y. J. Liu, Z. Liu, Neural-network-based adaptive leader-following consensus control for second-order non-linear multi-agent systems, *IET Control Theory Appl.*, **9** (2015), 1927–1934. https://doi.org/10.1109/TCYB.2016.2608499

36. S. S. Ge, C. C. Hang, T. Zhang, Adaptive neural network control of nonlinear systems by state and output feedback, *IEEE T. Syst. Man Cy. B*, **29** (1999), 818–828. http://dx.doi.org/10.1109/3477.809035

37. W. Yang, G. Cui, Q. Ma, J. Ma, C. Tao, Finite-time adaptive event-triggered command filtered backstepping control for a quav, *Appl. Math. Comput.*, **423** (2022), 126898. http://dx.doi.org/10.1016/j.amc.2021.126898
38. N. Koksal, H. An, B. Fidan, Backstepping-based adaptive control of a quadrotor uav with guaranteed tracking performance, *ISA T.*, **105** (2020), 98–110. http://dx.doi.org/10.1016/j.isatra.2020.06.006
39. K. Eliker, W. Zhang, Finite-time adaptive integral backstepping fast terminal sliding mode control application on quadrotor uav, *Int. J. Control Autom. Syst.*, **18** (2020), 415–430. http://dx.doi.org/10.1007/s12555-019-0116-3
40. F. Chen, L. Wen, K. Zhang, T. Gang, B. Jiang, A novel nonlinear resilient control for a quadrotor uav via backstepping control and nonlinear disturbance observer, *Nonlinear Dynam.*, **85** (2016), 1281–1295. https://link.springer.com/article/10.1007/s11071-016-2760-y

Appendix: Adaptive attitude control design of QUAV

According to Newton-Euler formula, the rotational dynamic can be depicted in the body fixed frame B as

$$\bar{I}\dot{\Omega}_a = -\Omega_a \dot{\times} \bar{I}\Omega_a + \tau, \tag{5.1}$$

where $\Omega_a = [\Omega_1, \Omega_2, \Omega_3]^T \in \mathbb{R}^3$ is the rotational speeds; $\dot{\times}$ denotes the vector product (and also is called as cross product); $\bar{I} = diag\{\bar{I}_x, \bar{I}_y, \bar{I}_z\} \in \mathbb{R}^{3\times 3}$ is the inertia matrix that is a positive definite constant matrix; $\tau = [\tau_{rol}, \tau_{pit}, \tau_{yaw}]^T \in \mathbb{R}^3$ is the control torque.

Let $\eta_1(t) = [\theta_{rol}(t), \theta_{pic}(t), \theta_{yaw}(t)]^T \in \mathbb{R}^3$ denote three Euler angles. By using the rotation matrix $R(\eta_1)$, the attitude dynamic (5.1) can be transformed from the body frame B to the inertial frame E as (referring to [8])

$$\begin{aligned} \dot{\eta}_1(t) =& \eta_2(t), \\ \dot{\eta}_2(t) =& f_a(\eta_1, \eta_2) + \Phi(\eta_1)\bar{I}^{-1}\tau, \end{aligned} \tag{5.2}$$

where

$$f_a(\eta_1, \eta_2) = -\Phi(\eta_1)\bar{I}^{-1}(\Phi^{-1}(\eta_1)\eta_2(t)\dot{\times}\bar{I}\Phi^{-1}(\eta_1)\eta_2(t)) + \dot{\Phi}(\eta_1)\Phi^{-1}(\eta_1)\eta_2(t),$$

$$\Phi(\eta_1) = \begin{bmatrix} 1 & s_{(\theta_{rol})}t_{(\theta_{pit})} & c_{(\theta_{rol})}t_{(\theta_{pit})} \\ 0 & c_{(\theta_{rol})} & -s_{(\theta_{rol})} \\ 0 & s_{(\theta_{rol})}se_{(\theta_{pit})} & c_{(\theta_{rol})}se_{(\theta_{pit})} \end{bmatrix},$$

and $t_{(\cdot)}$ and $se_{(\cdot)}$ are the abbreviations of trigonometric functions $\tan(\cdot)$ and $\sec(\cdot)$ respectively.

For assisting the QUAV position control, the attitude control is required to subject to the command signal vector $\eta_{re}(t) = [\phi_{re}(t), \theta_{re}(t), \psi_{re}(t)]^T$. In the command signal vector $\eta_{re}(t)$, its yaw command element $\psi_{re}(t)$ needs to be predefined, then the roll and pitch command angles can be generated from (3.2) as

$$\phi_{re}(t) = \arcsin\Big(\bar{m}\frac{U_1\sin(\psi_{re}) - U_2\cos(\psi_{re})}{u_p}\Big),$$

$$\theta_{re}(t) = \arctan\Big(\frac{U_1\cos(\psi_{re}) + U_2\sin(\psi_{re})}{U_3}\Big). \tag{5.3}$$

Define the tracking error variables as $e_{\eta 1}(t) = \eta_1(t) - \eta_{re}(t)$ and $e_{\eta 2}(t) = \eta_2(t) - \alpha_\eta$, where $\alpha_\eta \in \mathbb{R}^3$ is the virtual control. From (5.2), the error dynamics can be yielded as follows,

$$\begin{aligned} \dot{e}_{\eta 1}(t) =& \eta_2(t) - \dot{\eta}_{re}(t), \\ \dot{e}_{\eta 2}(t) =& f_a(\eta_1, \eta_2) + \Phi(\eta_1)\bar{I}^{-1}\tau - \dot{\alpha}_\eta, \end{aligned} \tag{5.4}$$

where $F(\eta_1, \eta_2, \dot{\alpha}_\eta) = f_a(\eta_1, \eta_2) - \dot{\alpha}_\eta$.

The QUAV attitude control is derived from 2-step backstepping as well. In the first backstepping step, the virtual control is designed as

$$\alpha_\eta = -\kappa_3 e_{\eta 1}(t) + \dot{\eta}_{re}(t), \tag{5.5}$$

where κ_3 is the design parameter with $\kappa_3 > 0$.

In the second backstepping step, the final QUAV attitude control is derived by using the adaptive NN in the following.

The NN is used to approximate the uncertain function $F(\eta_1, \eta_2, \dot{\alpha}_\eta)$ as

$$F(\eta_1, \eta_2, \dot{\alpha}_\eta) = \Psi_a^{*T}\varpi_a(\eta_1, \eta_2, \dot{\alpha}_\eta) + \epsilon_a, \tag{5.6}$$

where $\Psi_a^* \in \mathbf{R}^{m\times 3}$ is the optimal NN weight, $\varpi_a(\eta_1, \eta_2, \dot{\alpha}_\eta) \in \mathbf{R}^m$ is the basis function vector and $\epsilon_a \in \mathbf{R}^3$ is the approximation error.

Then the adaptive attitude control can be similarly designed with the position control (3.14) as

$$\tau = -\bar{I}\Phi^{-1}(\eta_1)(\kappa_4 e_{\eta 2}(t) + \gamma_a\hat{\psi}_a(t)\|\varpi_a(\eta_1, \eta_2, \dot{\alpha}_\eta)\|^2 e_{\eta 2}(t)), \tag{5.7}$$

and the adaptive parameter $\hat{\psi}_a(t) \in \mathbf{R}$ is updated via the following rule:

$$\dot{\hat{\psi}}_a(t) = \gamma_a\|\varpi_a(\eta_1, \eta_2, \dot{\alpha}_\eta)\|^2\|e_{\eta 2}(t)\|^2 - \beta_a\hat{\psi}_a(t), \tag{5.8}$$

where κ_4, γ_a and β_a are the positive design parameters and $\hat{\psi}_a(t)$ is the adaptive estimation of optimal NN weight's norm $\psi_a^* = \|\Psi_a^*\|^2$.

Since the stability proof of the attitude control is similar to the proof of Theorem 1, it is omitted here.